

To Balance or to Not? Battery Aging-Aware Active Cell Balancing for Electric Vehicles

Enrico Fraccaro^{1,3}, Seongik Jang², Logan Stach³, Hoeseok Yang⁴, Sangyoung Park⁵ and Samarjit Chakraborty³

¹University of Verona, Italy.

²Hyundai Motor Company, South Korea.

³University of North Carolina at Chapel Hill, NC, USA.

⁴Santa Clara University, CA, USA.

⁵Technical University of Berlin, Germany.

Abstract—Due to manufacturing variabilities and temperature gradients within an electric vehicle’s battery pack, the capacities of cells in it decrease differently over time. This reduces the usable capacity of the battery – the charge levels of one or more cells might be at the minimum threshold while most of the other cells have residual charge. Active cell balancing (i.e., transferring charge among cells) can equalize their charge levels, thereby increasing the battery pack’s usable capacity. But performing balancing means additional charge transfer, which can result in energy loss and cell aging, akin to memory aging in storage technologies due to writing. This paper studies when cell balancing should be optimally triggered to minimize aging while maintaining the necessary driving capability. In particular, we propose optimization strategies for cell balancing while minimizing their impact on aging. By borrowing terminology from the storage domain, we refer to this as “wear leveling-aware” active balancing.

Index Terms—Active Cell Balancing, Charge Equalization, Battery Management, Modeling, Simulation

I. INTRODUCTION

The widespread adoption of Electric Vehicles (EVs) faces a key challenge – battery aging [1], [2]. How to mitigate aging has attracted considerable attention since the battery is the most expensive component of an EV. Aging diminishes the charge retention capacity of cells and poses a problem in any Lithium-ion (Li-ion) battery pack [3]. Because of manufacturing variability and temperature gradient within a pack, its cells can age at different rates [4]. As a result, the charge level of cells in a pack can differ despite them all being subjected to the same charging and discharging current.

In the example of Fig. 1, an imbalanced battery pack is dealt with by using *cell balancing* [5]–[7], highlighting two key issues: (1) different maximum capacities of cells ($Q_{max,i}$) caused by manufacturing deviation or differential aging, and (2) different total charge in each cell (Q_i) at any time. Although in this example, every cell is charged or discharged at the same rate, because of the differences in their capacities $Q_{max,i}$, their charge levels are different at any point in time. One of the main consequences of such a charge imbalance is a *reduction in the usable capacity of the*

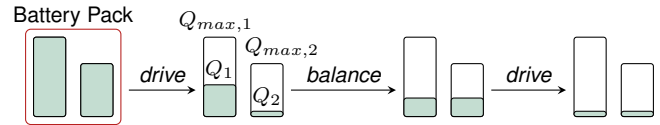


Figure 1. Example of battery usage, where *cell balancing* can increase the *driving range* of a typical battery pack.

battery pack. Fig. 1 illustrates the problem where, after the EV has driven for some time, the charge level of the second cell reduces to zero, while the first one still has charge left in it. Once the charge level of a cell goes below or above certain thresholds (e.g., below 20% or above 100%) [8], it should not be discharged or charged any further. Violating these thresholds might not have an immediate impact on the battery itself. Still, if repeated, it can lead to permanent changes in the electro-chemical properties of the battery and sub-optimal performances. Two solutions can extend the usage of the battery: (1) charging the pack or (2) transferring charges between cells so that all of them have some charge. The latter is known as *cell balancing* [9]–[11], and the objective is to equalize the State of Charge (SoC) between the cells of a pack. The SoC represents a cell’s charge level relative to its capacity and is expressed as a percentage.

Innovations in this paper: Where there is a considerable volume of work on developing optimal cell balancing strategies and architectures [12]–[15], active cell balancing comes at a price. Migrating charges causes energy loss and uneven aging of cells, decreasing their capacity and increasing charge imbalance. We should use it cautiously and do it on an *as-needed basis* to minimize its negative effect on aging instead of doing it at *every* opportunity. *When* should we trigger active cell balancing, and by *how much* should we balance the battery pack? These are non-trivial questions that previous studies have not addressed yet, and this paper aims to answer them. Towards this, we assume that the EV has to complete a *mission*, defined by the distances it travels, its times, and the amount of charging/discharging current. Given such a mission, our goal is to determine the balancing actions to accomplish it while minimizing the aging of the cells. Borrowing terminology from the storage technologies domain, we refer to this as *wear leveling-aware*, active cell balancing.

This study was supported by the NSF grant No. 2038960, and from the European Union’s Horizon Europe research and innovation program under the Marie Skłodowska-Curie grant No. 101109243. A preliminary version of this paper is due to appear in VLSI Design 2024.

This paper shows that determining the optimal balancing schedule is an optimization problem. The main contributions are formulating and solving this problem, which fills an essential gap in the active cell balancing literature. An assumption we make is the notion of a *mission* and our complete knowledge about it. We encourage the readers to see this as a foundational step towards solving the more general and realistic problem, where the “mission” is not entirely known, and its various components are only specified in a stochastic setting. The resulting stochastic optimization problem can be solved by leveraging the solution we propose in this paper.

II. BACKGROUND

Much literature exists on automotive embedded systems and software [16], [17]. While the issue of active power management arises in battery-operated devices [18]–[20], a different form of power management in combination with automotive embedded systems arises in electric vehicles. This section introduces this and outlines basic concepts related to battery aging and some prominent cell-balancing architectures. It then explains the non-neighbor active cell balancing architecture we rely upon.

A. Battery aging models

Aging-induced degradation of Li-ion batteries with usage is inevitable, and both external and internal factors can influence it. There are several approaches to model battery degradation, and in general, they fall into two categories: empirical [21] and electro-chemical [22] models. As the name implies, the former is a simple and effective model based on parameters fitted from extensive measurement data. The latter describes and mimics the underlying electrochemical processes that occur inside a battery during its lifetime. Section IV-A provides a detailed description of the model we rely upon in this paper, specifically, the empirical model presented in [21].

B. Cell balancing architectures and strategies

There are two prominent families of cell balancing architectures: *passive* and *active*. *Passive* balancing equalizes the SoC across cells by dissipating excess energy from cells to reach the charge level of the cell with the lowest SoC. Although simple, this strategy wastes energy that could instead be used for driving. It also increases the temperature of the pack and further accelerates aging (see [21] for more details). *Active* balancing equalizes SoC by migrating charge among cells. It is more advantageous and has been extensively studied in the literature recently. Follows a list of the most prominent active cell balancing architectures and strategies.

Depending on the energy storage element, we could consider several variations of the active cell balancing architectures in this work. There are three prominent families of architectures, i.e., capacitor-based [23], inductor-based [24], and transformer-based [25]. In this section, we first discuss a capacitor-based one, followed by an inductor-based one, and finally, we provide a lengthy description of a transformer-based one that we relied upon in this work. The approach in

this paper is compatible with any of these variations; we need access to the software controlling *when* balancing is activated.

In this paper, we rely upon a transformer-based architecture that enables exchanging charges between non-adjacent cells, improving balancing efficiency and time [25]. The proposed balancing architecture equips each cell with a balancing module composed of the flyback transformer and several switches. It then controls each switch, establishing a path for transferring charges from the source to the destination cell, passing through a temporary energy buffer. Thanks to its topology, charges can be physically transmitted and received simultaneously among multiple pairs of cells. With the term *single transfer cycle*, we refer to the time it takes for the software-based controller to operate the control signals that actuate the switches and transfer energy from one cell to another. The time it takes to perform the whole transfer operation is identified by 1) the charging of the first winding and 2) the transfer of the charges to the non-adjacent cell. Furthermore, the transfer time depends on the pair of cells involved in the operation (more details on this in Section V). For the remainder of the paper, we identify the time it takes to perform *single transfer cycle* from the i -th to the j -th cell with $T_c(i, j)$.

III. RELATED WORK

There are several balancing strategies for equalizing battery charges. [24] proposes an *inductor-based* balancing architecture that allows concurrent charge transfers between non-adjacent cells. It uses a heuristic-based balancing strategy that selects a set of charge transfer pairs and the appropriate architecture that enables those transfers. A *transformer-based* balancing architecture that enables concurrent charge transfers between non-adjacent cells is studied in [25]. Here, a hybrid balancing strategy transfers charges between individual cells and from a single cell to a group of cells and vice versa, with increased energy efficiency and low balancing time. [26] proposes an active balancing strategy focusing on minimizing energy loss and balancing time. While these strategies might achieve their objectives, they do not consider the aspects related to batteries’ State of Health (SoH). They all consider cells to be identical, disregarding the effect of manufacturing process deviation on the physical aspects of the batteries and, consequently, on balancing. In contrast, [27] considers cells with different charge/discharge rates and formulates a balancing strategy that compensates for it. It extends the usable time when discharging and reduces the charging time through preconditioning. However, its primary goal is to extend the battery’s usable capacity, and it does not aim to minimize the impact on cell aging.

Other studies propose SoH-aware cell balancing strategies. Recently, [28] described an active cell balancing strategy that extends battery pack lifespan by mitigating the thermal gradient inside the pack. However, it considers an abstracted balancing behavior without concrete consideration of actual balancing operations. [29] proposes a heuristic-based active cell balancing. After studying the aging model, it concludes that letting weaker cells rest can extend the battery pack’s

lifespan. It proposes a balancing strategy where healthier cells help the other ones discharge less load current. However, it assumes a simplified balancing operation instead of a realistic transferring process. The heuristic strategy cannot be based on a quantitative optimization of charge transfer.

This paper proposes an optimized balancing strategy based on the quantitative model of the imbalance evolution over time, with an analytic model of the balancing operation.

IV. SYSTEM MODEL

This section shows the model of the batteries, the driving profile we use to formulate our optimal balancing strategy and our analytic model of active cell balancing architecture.

A. Battery Model

In this paper, we consider the typical battery pack mounted on EVs, consisting of 96 series-connected modules, and each module is composed of 24 parallel connected cells. Let us assume that the parallel cells are electronically indistinguishable, so the charging and discharging currents are evenly distributed between parallel cells. Ideally, each manufactured cell has a nominal capacity of 2.5 Ah; however, it eventually differs from the nominal value due to different factors, from manufacturing process variation to aging. The ratio of the current maximum capacity of a cell to the nominal one of a new cell is a good indicator of its degree of aging, thus called SoH, and is expressed as a percentage.

Self-discharging is a chemical phenomenon that causes batteries to lose charge even when not connected to an electrical load. These are usually called self-discharging currents and are the main reason for charge imbalance inside battery packs [30]. Furthermore, Li-ion battery cells are known to charge and discharge at different rates [31], which represents another source of imbalance. Throughout this paper, we denote with $Q_{max,i}$ the nominal capacity of the i -th cell and its remaining charge with Q_i while we denote its self-discharge current with $I_{sr,i}$. Charge and discharge rates are denoted as $\eta_{c,i}$ and $\eta_{d,i}$, respectively, and describe the efficiency by which electrons are transferred from and to the cells.

The battery degrades with repeated charge and discharge cycles. We can compute the percentage of capacity lost during the lifetime of the i -th cell as follows [21]:

$$Q_{loss,i} = a \cdot e^{b \cdot C_{rate,i}} \cdot Ah_{thrp,i}, \quad (1)$$

where $C_{rate,i}$ is the measured ratio of current to the maximum capacity, and $Ah_{thrp,i}$ is the amount of charged and discharged current. Meanwhile, a and b are tunable temperature-dependent coefficients. Section V explains how both $C_{rate,i}$ and $Ah_{thrp,i}$ are computed. We can compute the effect of aging on the SoH for the i -th cell as follows:

$$SoH_i [\%] = 100 - Q_{loss,i}. \quad (2)$$

When the SoH reaches 80% (i.e., we have lost more than 20%), the battery is considered to be in its end-of-life state (or second-life state) [32]. Ideally, it becomes inefficient if installed on an EV; however, these second-life batteries still have some use in non-automotive applications.

B. Driving Profile Model

We consider the driving profile (mission) as a finite list of n segments, each representing the current usage and its length in terms of time. The current usage can be any of three among discharging ($I > 0$), charging ($I < 0$), and idle current ($I = 0$). We can formally describe the driving profile as a sequence of tuples as follows:

$$\mathcal{M} = \langle \langle I_1, t_0, t_1 \rangle, \dots, \langle I_k, t_{k-1}, t_k \rangle, \dots, \langle I_n, t_{n-1}, t_n \rangle \rangle, \quad (3)$$

where I_k is the current usage during the whole segment, while t_{k-1} and t_k are the starting and ending times of the k -th segment, respectively. Without loss of generality, we assume that the current usage inside a segment remains constant. Nevertheless, we can consider varying currents by splitting a segment into smaller segments with different current usages. Given a mission, we can model the current usage at time t as a piecewise constant function as follows:

$$I(t) = I_k \mid t_{k-1} \leq t < t_k. \quad (4)$$

We can formulate the remaining charge amount of the i -th cell after the k -th segment as follows:

$$Q_i^k = Q_i^0 - \int_0^{t_k} (\eta_i \cdot I(t) + I_{sr,i}) dt, \quad (5)$$

where η_i is $\eta_{c,i}$ when we are charging, $\eta_{d,i}$ when we are discharging, or 0 when idle.

C. Analytic Model of Active Cell Balancing

Several active cell balancing architectures exist, as discussed in Section II. This paper uses the balancing architecture proposed in [25], which enables concurrent charge transfers between non-neighbor cells within the maximum distance d . The value d is computed based on the voltage the switches composing the architecture can withstand. Although concurrent charge transfer is possible, balancing paths cannot overlap between multiple pairs as it would cause a short circuit. The following equations are *inspired* by the work in [26], and we *refine* them to enable the novel formulation of Section V.

The transmitted charge from the i -th cell to another one during a single transfer operation is computed as follows:

$$Q_{tx}(i) = \ln \left(\frac{V_i}{V_i - I_{peak} \cdot R_s(i)} \right) \cdot \frac{L \cdot V_i}{R_s(i)^2} - \frac{L \cdot I_{peak}}{R_s(i)}, \quad (6)$$

where V_i is the voltage of the i -th cell, $R_s(i)$ is the parasitic resistances of the circuit around it, L is the inductance of the secondary winding of the transformer, and I_{peak} denotes the peak current that flown through it. Specifically, $R_s(i)$ considers the source cell resistance, the parasitic resistances of its winding, and the parasitic resistances of its switches.

The amount of charge that the i -th cell receives from the j -th one in a single transfer operation is computed as follows:

$$Q_{rx}(i,j) = \ln \left(\frac{V_i}{V_i + I_{peak} \cdot R_d(i,j)} \right) \cdot \frac{L \cdot V_i}{R_d(i,j)^2} + \frac{L \cdot I_{peak}}{R_d(i,j)}, \quad (7)$$

where $R_d(i,j)$ is the total resistance in the path from the receiving cell i to the source cell j and is directly proportional to the distance between them. Specifically, $R_d(i,j)$ considers the source cell resistance, the parasitic resistances of its winding, and all the parasitic resistances of the switches encountered on

the path. It does not include the destination cell's resistance, which is already considered by $R_s(i)$.

V. BALANCING METHODOLOGY

This section proposes our balancing strategy accounting for different cell capacities, called *wear leveling-aware* active cell balancing. This strategy aims to minimize unnecessary balancing operations based upon a limited knowledge of our future missions, i.e., only for a given time window. Conversely, the state-of-the-art balancing strategy proposed in [26], which we call *opportunistic* balancing, assumes to equalize the charge of cells at every opportunity, regardless of future missions.

The baseline for comparing balancing strategies is the *no balancing* approach, which has no impact on the aging of the cells. While *opportunistic* balancing instead exploits every single *idle* period to balance the SoC of the cells. It effectively keeps the charge levels equalized at all times but leads to accelerated aging of the cells. However, *wear leveling-aware* balancing delays the balancing operation and performs it only when necessary, i.e., when the SoC of some cells is about to go below 20% during the next drive activity. We can also set a higher threshold to increase our safety margin.

To summarize the effect of each strategy on aging. The baseline is the *no-balancing* strategy, which has a low impact on aging, but we might not be able to complete our mission with it. *Wear leveling-aware* balancing speeds up aging and ensures we can complete future missions. Similarly, *opportunistic* ensures we can complete future missions at the expense of faster aging. This paper wants to find the trade-off between the two opposing strategies.

A. Wear leveling-aware balancing

In this paper, we propose an optimal way to perform balancing that guarantees fulfilling the foreseen future missions when we know the details of the next day's mission. The idea is to receive the details of the next day's mission during the night, i.e., when the vehicle is inactive and probably charging.

We have already established that we cannot further discharge serially connected cells when even one of them runs out of charge. The *usable capacity*, namely Q_{UC} , can be defined as the minimum remaining charge between cells. When we know the mission for the following day, we can quantitatively calculate the remaining charge of each cell after each discharge activity by using Eq. (5). Due to the different self-discharge currents and nominal capacities, the imbalance may get exacerbated, making the following activities unachievable without balancing. In some cases, we would need to perform balancing during idle segments. The set of indices of idle segments up to the k -th segment can be defined as follows:

$$\mathcal{L}_k = \{l | 1 \leq l \leq k, I_l = 0\}. \quad (8)$$

While the voltage levels of cells are assumed to remain constant during a single balancing event, they may vary between balancing events as the charge level may vary severely according to usage. The analytic models of transmitted and received charges shown in Eqs. (6) and (7) must be extended to

account for different voltage levels at different idle segments. As such, we need to change them as follows:

$$Q_{tx}^l(i) = \ln \left(\frac{V_i^l}{V_i^l - I_{peak} \cdot R_s(i)} \right) \cdot \frac{L \cdot V_i^l}{R_s(i)^2} - \frac{L \cdot I_{peak}}{R_s(i)}, \quad (9)$$

$$Q_{rx}^l(i, j) = \ln \left(\frac{V_i^l}{V_i^l + I_{peak} \cdot R_d(i, j)} \right) \cdot \frac{L \cdot V_i^l}{R_d(i, j)^2} + \frac{L \cdot I_{peak}}{R_d(i, j)}. \quad (10)$$

Before building our constraints, we need to define our **decision variable** $CT_{i,j}^l$, which denotes the number of transfer operations from the i -th cell to the j -th during the l -th idle period. Notably, the amount of charge transmitted and received depends on the distance between the pairs of cells and their voltages. The cell voltage is proportional to the SoC of cells. In this paper, we assume that cell voltage remains constant during the balancing process as the difference in charge is negligible [26]. We also assume that the balancing operations happen only when the pack is not utilized, i.e., during the idle periods. We define P_i as the set of "compatible" cells that can either receive from or transmit to the i -th cell, i.e., those within the maximum distance d . We can start building our first constraint by computing each cell's total transmitted and received charges during each idle period.

The total transmitted charges from the i -th cell to all the other compatible cells in the l -th idle period is computed as:

$$Q_{T,i}^l = \sum_{j \in P_i} (Q_{tx}^l(i) \cdot CT_{i,j}^l), \quad (11)$$

while the charge the i -th cell receives is computed as follows:

$$Q_{R,i}^l = \sum_{j \in P_i} (Q_{rx}^l(i, j) \cdot CT_{j,i}^l). \quad (12)$$

The act of balancing inherently changes the charge level of the cells. We can compute the charge level of the i -th cell after balancing at the k -th segment, as follows:

$$\overline{Q}_i^k = Q_i^k + \sum_{l \in \mathcal{L}_k} (Q_{R,i}^l - Q_{T,i}^l). \quad (13)$$

After a balancing operation, the charge levels must be sufficient for upcoming driving activities but always stay within safe ranges. This means they must be *higher* than the minimal usable capacity and *lower* than the maximum nominal capacity. As such, we can formulate our first balancing constraint as follows:

$$\forall i, k, Q_{UC} \leq \overline{Q}_i^k \leq Q_{max,i}. \quad (14)$$

Here k is unbounded (i.e., $\forall k$); however, in the objective function, k will be set to the size of our *knowledge window*.

As mentioned in Section II-B, the time needed to perform a *single transfer cycle*, namely T_c , depends on the specific pairs of cells selected for the operation. We can compute the time it takes for the i -th cell to receive charges from the other compatible cells during the l -th idle period as follows:

$$T_{tran,i}^l = \sum_{j \in P_i} (CT_{j,i}^l \cdot T_c(j, i)), \quad (15)$$

where $T_c(j, i)$ is the specific *single transfer cycle* time between cells j and i . In general, the balancing time is given by the number of *single transfer cycles* it takes each feasible pair of cells to perform charge equalization. Here, we perform balancing during idle periods; thus, we must constrain the

balancing time to complete within those periods. This means that the balancing time during the l -th idle period must be lower than the length of the idle period Δ_l . We can write our second balancing constraint as follows:

$$\forall l \in \mathcal{L}_k, \sum_i T_{tran,i}^l \leq \Delta_l. \quad (16)$$

After defining these two constraints, we build our objective function to be minimized. The battery's throughput up to the k -th segment, defined as the sum of absolute charged and discharged current, can be computed by treating the balancing as micro-charging or micro-discharging events as follows:

$$Ah_{thrp,i}^k = \int (\eta_i \cdot |I(t)| + I_{sr,i}) dt + \sum_{l \in \mathcal{L}_k} (Q_{T,i}^l + Q_{R,i}^l). \quad (17)$$

While the ratio of average current to maximum capacity up to the k -th segment is defined as:

$$C_{rate,i}^k = \frac{Ah_{thrp,i}^k}{Q_{max,i} \cdot T}, \quad (18)$$

where T is the cumulative usage time up to the k -th segment.

It would seem appropriate to minimize the capacity loss of the i -th cell by using Eq. (1). However, since the aging model exhibits non-linear behavior, the objective function cannot be directly formulated in a linear form by using Eq. (1). Instead, we have seen after extensive study that $C_{rate,i}^k$ is a monotonically increasing function of $Ah_{thrp,i}^k$, and the capacity loss is also a monotonically increasing function of $Ah_{thrp,i}^k$. We can use $Ah_{thrp,i}^k$ in the formulation to maintain linearity instead of directly using Eq. (1). Finally, we can build our optimization function to minimize the maximum degradation among the cells (i.e., wear leveling) for a given time window w . When the number of mission segments for the next day is w , we can limit the range of values that k can assume, and the *wear leveling-aware* balancing objective can be formulated as follows:

$$\text{Min} \left(\max(Ah_{thrp,i}^k) \right), \quad (19)$$

s.t. $\forall i, t \leq k \leq t + w$, Eqs. (14) and (16) hold true,

where the current time is t , and w is the size of our *knowledge window*. We write the optimization problem described above as an Mixed Integer Linear Programming (MILP) formulation. Its solution yields the number of charge transfer operations during idle periods $CT_{i,j}^l$, equalizing cells wear.

VI. EXPERIMENTAL SETUP AND RESULTS

This section compares our proposed *wear leveling-aware* strategy against the state-of-the-art *opportunistic* one in typical real-world scenarios. Our simulation environment is written in Python, while we use CPLEX [33] to solve the MILP problem, with a timeout of 5 s for finding a solution. If the optimizer takes more than 5 s to complete, we return the initial charge distribution as a result (i.e., no balancing). This is necessary because the *opportunistic* strategy tends to run for long periods, leading to simulations that last for hours.

We consider the peak current I_{peak} for our battery pack to be 12 A, and the maximum distance between cells can exchange charge d is 6. We use the aging model shown in

Eq. (1) and set the temperature of the cells to 22 °C for all experiments. We interpolate parameters a and b for the 22 °C temperature, based upon the values proposed in [21], and obtain $a = 0.00083$ and $b = 0.3789$. To model manufacturing process variation for our 2.5 Ah cells, we generate their nominal capacities following a normal distribution with a mean of 100% and a standard deviation of 4% [34]. We have also randomly generated each cell's self-discharge currents, charge, and discharge rates following a normal distribution. Specifically, we uniformly distribute charge and discharge rates in relatively small ranges with $\eta_c \in [0.996, 1.00]$ and $\eta_d \in [1.00, 1.001]$, since Li-ion batteries are known to have high efficiency [31]. On the other hand, since self-discharge currents are the leading causes of imbalance, we assume they follow a normal distribution with a mean of 0.175 mA and a standard deviation of 0.1 mA. Even when the battery is not utilized, part of its charge is depleted because of the self-discharge phenomenon. We set the minimum usable capacity Q_{UC} as 20% of the total capacity [8].

To compare the balancing algorithms extensively, we generated 50 scenarios with the following procedure. First, we randomly generate a connected Watts–Strogatz small-world graph with 30 nodes, each connected with six nearest neighbors, and a 30% probability of rewiring each edge (see [35] for a detailed explanation). Then, we randomly generate travel times and currents for each edge, select four nodes as charging stations, and generate probability distributions for the outgoing edges of each node. We generate our missions by simulating thousands of random walks of length 10, starting from a node marked as a charging station. That ensures we can charge the battery at least once during our missions. We place an idle period with a randomly generated duration between segments.

Solving an optimization problem can be both time-consuming and energy-intensive. This could be problematic if the algorithm that solves it is meant to be used in an embedded setup. As such, it is essential to assess both the time taken and the memory used by the different balancing techniques. Before discussing the results, it is worth clarifying that the *opportunistic* strategy runs at every idle period. In contrast, the *wear leveling-aware* one is executed only once at the start of the knowledge window. The algorithm can work with knowledge windows ranging from knowing the next driving segment to knowing the entire day or several. As such, the size of the knowledge window determines how many times the *wear leveling-aware* optimization runs. Table I reports the peak memory usage and the elapsed time required to solve each optimization problem, with *wear leveling-aware* having

Table I
MINIMUM, MAXIMUM, AND AVERAGE PEAK MEMORY USAGE AND SOLVE TIME FOR EACH BALANCING TECHNIQUE.

Algorithm	Peak Memory (KB)			Solve time (ms)		
	Min	Avg	Max	Min	Avg	Max
Opportunistic	2	28	561	33	2472	5489
Wear leveling-aware	69	71	176	64	79	1268

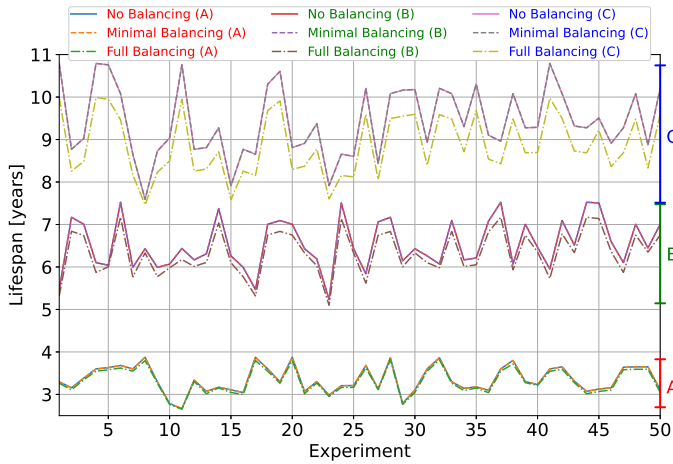


Figure 2. Comparing battery lifespan with *none*, *opportunistic* and *wear leveling-aware* (WLA) balancing strategies.

a knowledge window of one day. Both strategies have low average memory usage, making both viable solutions for an embedded system platform. The *Opportunistic* strategy takes considerably more time to find a solution than the *wear leveling-aware* one. The average solve time for *opportunistic* balancing would have been even higher if we did not set a 5 s timeout inside the CPLEX solver. The *opportunistic* strategy has a broader range of performance metrics, while the *wear leveling-aware* one has a narrower range. These results show how the *wear leveling-aware* strategy has lower variability with comparable if not better results than the *opportunistic* one, making it a more reliable and compelling solution.

Next, we evaluated the impact of each balancing strategy on the lifespan. We are comparing the lifespan, in each mission, when the car is used every day (A), once every two days (B), and once every three days (C). This sums up to a total of 150 simulations and comparisons. The comparison between the three strategies is depicted in Fig. 2. The *wear leveling-aware* strategy has the same lifespan as **not doing balancing** in all scenarios. When comparing the *wear leveling-aware* against the *opportunistic*, the improvements are, on average, one month with scenario A, four and a half months with scenario B, and around ten months with scenario C. Although all experiments are substantially different from each other, *wear leveling-aware* can improve the lifespan in every one of them. Let's compare the average number of balancing operations of *wear leveling-aware* against the *opportunistic*. It is 7 against 842 in scenario A, it is 3 against 420 in scenario B, and it is 3 against 284 in scenario C. As expected, *wear leveling-aware* drastically reduces the number of balancing operations. Overall, *wear leveling-aware* has better performances in terms of reduced aging, memory consumption, and solving time, making it a compelling cell balancing strategy.

VII. CONCLUDING REMARKS

This paper presents an active cell balancing strategy, viz., when and how much we balance, that optimally triggers balancing to minimize aging from balancing. We compared this *wear leveling-aware* strategy against a more intuitive

opportunistic strategy. Results show that our approach ensures we can complete a planned driving mission while having a negligible impact on aging from balancing. Although both strategies have a low impact on memory usage, *opportunistic* balancing takes considerably more time and often fails to solve. Furthermore, our approach is compatible with different cell aging models and balancing architectures. Future investigations will study (1) stochastic modeling of future driving patterns to replace the current oracle-like knowledge of them, (2) include dynamic evolution of cell temperature based upon thermal modeling and simulation, and (3) testing the aging evolution with other optimization objectives.

REFERENCES

- [1] S. Chakraborty *et al.*, "Embedded systems and software challenges in electric vehicles," in *Design, Automation & Test in Europe Conference (DATE)*, 2012.
- [2] G. Georgakos *et al.*, "Reliability challenges for electric vehicles: from devices to architecture and systems software," in *50th Annual Design Automation Conference (DAC)*, 2013.
- [3] S. Park, L. Zhang, and S. Chakraborty, "Battery assignment and scheduling for drone delivery businesses," in *International Symposium on Low Power Electronics and Design (ISLPED)*, 2017.
- [4] T. Baumhöfer *et al.*, "Production caused variation in capacity aging trend and correlation to initial cell performance," *Journal of Power Sources*, vol. 247, pp. 332–338, Feb. 2014.
- [5] M. Kauer, S. Narayanaswamy, S. Steinhorst, and S. Chakraborty, "Rapid analysis of active cell balancing circuits," *IEEE Trans. Comput. Aided Des. Integr. Circuits Syst.*, vol. 36, no. 4, pp. 694–698, 2017.
- [6] S. Narayanaswamy, S. Park, S. Steinhorst, and S. Chakraborty, "Multi-pattern active cell balancing architecture and equalization strategy for battery packs," in *International Symposium on Low Power Electronics and Design (ISLPED)*, Jul. 2018.
- [7] S. Narayanaswamy, S. Steinhorst, M. Lukasiewicz, M. Kauer, and S. Chakraborty, "Optimal dimensioning and control of active cell balancing architectures," *IEEE Trans. Veh. Technol.*, vol. 68, no. 10, pp. 9632–9646, 2019.
- [8] V. J. Ovejias and A. Cuadras, "State of charge dependency of the overvoltage generated in commercial Li-ion cells," *Journal of Power Sources*, vol. 418, pp. 176–185, Apr. 2019.
- [9] D. Roy, S. Narayanaswamy, A. Probstl, and S. Chakraborty, "Multi-stage optimization for energy-efficient active cell balancing in battery packs," in *IEEE/ACM International Conference on Computer-Aided Design (ICCAD)*, IEEE/ACM, IEEE, Nov. 2019, pp. 1–8.
- [10] M. Kauer, S. Narayanaswamy, S. Steinhorst, M. Lukasiewicz, and S. Chakraborty, "Many-to-many active cell balancing strategy design," in *20th Asia and South Pacific Design Automation Conference (ASP-DAC)*, 2015.
- [11] M. Kauer, S. Narayanaswamy, M. Lukasiewicz, S. Steinhorst, and S. Chakraborty, "Inductor optimization for active cell balancing using geometric programming," in *Design, Automation & Test in Europe Conference & Exhibition (DATE)*, 2015.
- [12] S. Narayanaswamy, S. Park, S. Steinhorst, and S. Chakraborty, "Design automation for battery systems," in *International Conference on Computer-Aided Design (ICCAD)*, 2018.
- [13] S. Steinhorst, M. Kauer, A. Meeuw, S. Narayanaswamy, M. Lukasiewicz, and S. Chakraborty, "Cyber-physical co-simulation framework for smart cells in scalable battery packs," *ACM Trans. Design Autom. Electr. Syst.*, vol. 21, no. 4, pp. 62:1–62:26, 2016.
- [14] S. Steinhorst *et al.*, "Distributed reconfigurable battery system management architectures," in *21st Asia and South Pacific Design Automation Conference (ASP-DAC)*, 2016.
- [15] S. Narayanaswamy, S. Steinhorst, M. Lukasiewicz, M. Kauer, and S. Chakraborty, "Optimal dimensioning of active cell balancing architectures," in *Design, Automation & Test in Europe Conference & Exhibition (DATE)*, 2014.
- [16] S. Chakraborty *et al.*, "Automotive cyber-physical systems: A tutorial introduction," *IEEE Des. Test*, vol. 33, no. 4, pp. 92–108, 2016.

- [17] W. Chang and S. Chakraborty, "Resource-aware automotive control systems design: A cyber-physical systems approach," *Found. Trends Electron. Des. Autom.*, vol. 10, no. 4, pp. 249–369, 2016.
- [18] N. Peters *et al.*, "Web browser workload characterization for power management on HMP platforms," in *11th International Conference on Hardware/Software Codesign and System Synthesis (CODES)*, 2016.
- [19] Y. Gu and S. Chakraborty, "A hybrid DVS scheme for interactive 3d games," in *14th IEEE Real-Time and Embedded Technology and Applications Symposium (RTAS)*, 2008.
- [20] —, "Power management of interactive 3d games using frame structures," in *21st International Conference on VLSI Design*, 2008.
- [21] J. Wang *et al.*, "Degradation of lithium ion batteries employing graphite negatives and nickel-cobalt-manganese oxide+spinel manganese oxide positives: Part 1, aging mechanisms and life estimation," *Journal of Power Sources*, vol. 269, pp. 937–948, Dec. 2014.
- [22] X. Jin *et al.*, "Physically-based reduced-order capacity loss model for graphite anodes in Li-ion battery cells," *Journal of Power Sources*, vol. 342, pp. 750–761, Feb. 2017.
- [23] A. C. Baughman and M. Ferdowsi, "Double-Tiered Switched-Capacitor Battery Charge Equalization Technique," *IEEE Transactions on Industrial Electronics*, vol. 55, no. 6, pp. 2277–2285, Jun. 2008.
- [24] M. Kauer *et al.*, "Modular system-level architecture for concurrent cell balancing," in *50th Annual Design Automation Conference (DAC)*, 2013.
- [25] S. Narayanaswamy, M. Kauer, S. Steinhorst, M. Lukaszewycz, and S. Chakraborty, "Modular active charge balancing for scalable battery packs," *IEEE Transactions on Very Large Scale Integration (VLSI) Systems*, vol. 25, no. 3, pp. 974–987, Mar. 2017.
- [26] D. Roy *et al.*, "Optimal scheduling for active cell balancing," in *IEEE Real-Time Systems Symposium (RTSS)*, 2019.
- [27] A. Lamprecht *et al.*, "Enhancing battery pack capacity utilization in electric vehicle fleets via SoC-preconditioning," in *22nd Euromicro Conference on Digital System Design (DSD)*, 2019.
- [28] P. Kremer *et al.*, "Active cell balancing for life cycle extension of Lithium-ion batteries under thermal gradient," in *International Symposium on Low Power Electronics and Design (ISLPED)*, 2021.
- [29] A. Pröbstl *et al.*, "SOH-aware active cell balancing strategy for high power battery packs," in *Design, Automation & Test in Europe*, 2018.
- [30] D. Andrea, *Battery management systems for large lithium-ion battery packs*. Artech house, 2010.
- [31] F. Yang *et al.*, "A study of the relationship between coulombic efficiency and capacity degradation of commercial lithium-ion batteries," *Energy*, vol. 145, pp. 486–495, 2018.
- [32] B. Balagopal and M.-Y. Chow, "The state of the art approaches to estimate the state of health (SOH) and state of function (SOF) of lithium Ion batteries," in *13th Intl. Conf. Industrial Informatics (INDIN)*, 2015.
- [33] IBM, "ILOG CPLEX Optimization Studio version: 12.9.0," 2019. [Online]. Available: <https://www.ibm.com/docs/en/icos/12.9.0>
- [34] M. Dubarry, N. Vuillaume, and B. Y. Liaw, "From single cell model to battery pack simulation for Li-ion batteries," *Journal of Power Sources*, vol. 186, no. 2, pp. 500–507, Jan. 2009.
- [35] D. J. Watts and S. H. Strogatz, "Collective dynamics of 'small-world' networks," *Nature*, vol. 393, no. 6684, pp. 440–442, Jun. 1998.